Basic Properties of Cement Paste Mixed with Calcium Hydroxide-Ettringite Composite-Type Expansive Additive

Kohsuke Handa

Abstract

In this study, we targeted a calcium hydroxide and ettringite composite-type expansive additive (EA) and obtained the basic characteristics of the EA mixed cement paste in order to create a method for calculating volume expansion based on the hydration reaction of a PC-EA system. Expansion strain, setting time, and compressive strength were measured. In addition, we observed the state of the EA after hydration using a micro-CT scanner and scanning electron microscope, and elucidated the expansion mechanism.

Our results show that strain rapidly increased and compressive strength decreased when the replacement ratio of the EA (C_{rep}) exceeds 6.4%. At the same time, radial cracks were generated from the hydrated EA particles, suggesting that the EA itself grew to expand the cement paste. Although no ettringite was confirmed inside the EA when the C_{rep} was 5.1%, when the C_{rep} was 10.3%, ettringite was formed vertically from the surface of C_3A with a large amount of pores. These results show that simultaneous formation of ettringite and pores causes rapid expansion.

Keywords: Expansive additive, Calcium hydroxide, Ettringite, Micro-CT scanning, SEM

§1. INTRODUCTION

In order to maintain the durability and aesthetics of reinforced concrete structures over a long period of time, it is necessary to prevent the occurrence of cracks such as drying shrinkage cracking. For example, reducing drying shrinkage strain is effective in preventing cracks, and expansive additive (EA) can be used for this purpose. Although there are many types of EA, calcium hydroxide-ettringite composite-type EA is an admixture for concrete that has long been used, and its components are mainly composed of free-lime (f-CaO), anhydrite (CS), and hydraulic minerals such as calcium aluminate (C_3A) or calcium aluminoferrite (C_4AF) [1]. These minerals change into calcium hydroxide (CH) and ettringite (AFt) respectively. They have a large volume evolution, and thus give a cement paste (CP) a macroscopic volume expansion that compensates for shrinkage.

Up to now, regarding studies on the volume change mechanism of CP mixed with EA, Yamamoto et al. proposed the radius evolution of the EA from measurement data such as the reaction degree of each mineral and volume of CH and AFt [2]. In addition, Choi calculated the expansion strain of CP by mathematical modeling based on Yamamoto's data [3]. However, some challenges remain, such as that the radius evolution proposed by Yamamoto is not a value calculated based on the chemical reaction formula, and the particle size distribution is not taken into consideration.

This study aims to create a method for calculating the volume expansion of CP based on the hydration reaction and radius evolution of the calcium hydroxide-ettringite composite-type EA. In this study, experiments were conducted to measure the basic properties of CP mixed with EA. These included expansion strain, setting time, compressive strength, and static modulus of CP mixed with EA. In addition, the state of EA after hydration was observed using a micro-CT scanner and scanning electron microscope (SEM) to elucidate the expansion mechanism.

§2. EXPERIMENTS – TESTING METHODS

2.1 Sample preparation

All samples were prepared using moderate-heat Portland cement (PC) adapted JIS R 5210 [4] as Japanese standard, EA (powder), Polycarboxylic acid-based super plasticizer (Ad), and deionized water. The water-binder ratio was 0.45. The applied CP mix design is shown in Table 1. All samples were cured at room temperature (20 °C). The CP for micro-CT scanning and SEM was casted in a cylindrical resin bottle with 24 mm diameter and 39 mm height.

2.2 Setting time

In the expansion by EA, the force caused by this expansion is, unless it is a completely enclosed space, transmitted to the rebar or restrained member only when the mortar matrix is hardened and transmits the expansion pressure. That is, even if the unhardened paste expands, no stress is generated, so that it has no meaning within the structural design. Therefore, in this study, we focused on the expansion that occurs after hardening of CP begins.

The modified initial setting time determined by the modified Vicat Needle Test was adopted for the starting age of hardening. Instead of the water-cement ratio that produces the "normal consistency" paste proposed in JIS R 5201 [5], the water-binder ratio was kept constant at 0.45 and the test was conducted. This standard is almost the same as ASTM C191-13 [6], with slightly different conditions. The diameter of the

Table 1: Mix design for cement paste specimen and compressive strength

Name	Replacement ratio for cement Crep	Water-Binder ratio	Composition					Compressive strength		
			Water	PC	EA	Ad		[MPa]		
	(weight.%)	(%)	(g/L)	(g/L)	(g/L)	(mL/L)	(B×%)	1 day	3 days	7 days
Reference	0%	45%	590.9	1313.2	0.0	7.2	0.55	4.42	12.1	21.7
EA26	2.57%		590.6	1278.7	33.7			3.97	14.2	23.8
EA51	5.14%		590.3	1244.3	67.5			5.71	15.6	23.6
EA64	6.43%		590.2	1227.2	84.3			6.98	14.1	23.7
EA103	10.29%		589.7	1175.7	134.8			4.10	8.7	13.2
EA109	10.93%		589.6	1167.1	143.2			5.11	8.4	11.7
EA129	12.86%		589.4	1141.4	168.4			Not conducted		

needle for initial setting is 1.13 mm. For the modified initial setting time, the material age when the penetration depth of the Vicat needle was 1 mm from the bottom was adopted.

2.3 Expansion strain

Expansion strain of CP is measured using a 50 x 400 (x-axis direction) x 10 mm specimen. A 10-mm-square aluminum bar was installed to the end of the specimen, and the change in length of x-axis was measured by a non-reaction force LVDT. In order to reduce the frictional force, the CP was casted into a polyester film and a Teflon sheet was installed between the form on the bottom and the specimen.

2.4 Compressive strength

Compressive strengths were measured using a cylindrical specimen of 50 (diameter) x 100 (height) mm. 24 hours after casting, the CP specimens were carefully removed from their plastic molds, sealed in polyethylene plastic film.

2.5 Observation by micro-CT scanning

Slices with a thickness of 2-3 mm were cut from the sample in a resin bottle and then ground using a thin sectioning machine. Next, a micro-dicing machine was used and slices were processed into square bars. The length of each bar was approximately 0.92 to 1.02 mm. The bars were immersed in isopropanol until testing. Phoenix Nanotom m was used for the test.

2.6 Observation and elemental analysis by E-SEM

At 3 days of age, the sample was crushed with a hammer to a size of about 5-10 mm, and hydration was stopped with liquid nitrogen. The sample was immediately placed in a freeze-dryer and dried for 1 month. One month later, the sample was impregnated with epoxy resin while performing vacuum defoaming and cured. After the resin had hardened, each sample was grinded and polished on a lapping table with 6 μm, 3 μm, 1 μm, and 0.25 μm diamond paste. In between each paste, the samples were submerged in ethanol and ultrasonicated to remove debris. Following polishing, samples were kept in a desiccator until testing. Philips XL 30 ESEM was used for testing.

§3. EXPERIMENTS - RESULTS

3.1 Setting time

Test results of setting time are shown in Fig. 1. The setting time tended to be faster when the C_{rep} was up to 6.4%, but when the C_{rep} exceeded 6.4%, the setting time became slower as the C_{rep} increased.

3.2 Expansion strain

Test results of expansion strain at 7 days of age are shown in Fig. 1. For all strains, the strain at the modified initial setting time was set to 0. The strain increases sharply when the replacement ratio of EA (C_{rep}) exceeds 6.4%.

Fig. 2 shows the percentage of strain for each age when the expansion strain at 7 days is set to 100%. It can be seen that the percentage of expansion strain up to 0.5 day on the whole is different between the C_{rep} up to 6.4% and higher than that. This result shows that the reaction mechanism changes depending on the replacement ratio.

3.3 Compressive strength

Test results of compressive strength at 1 day, 3 days, and 7 days of age are shown in Table 1 and strength ratio compared to reference is shown in Fig. 3. Compressive strength tended to decrease when the C_{rep} exceeded 6.4%.

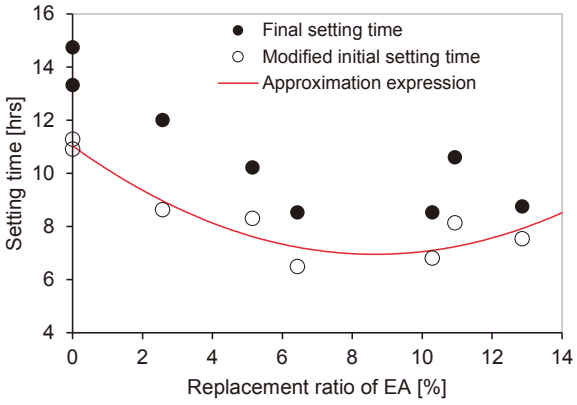

Figure 1: Relationship between C_{rep} and modified initial setting time

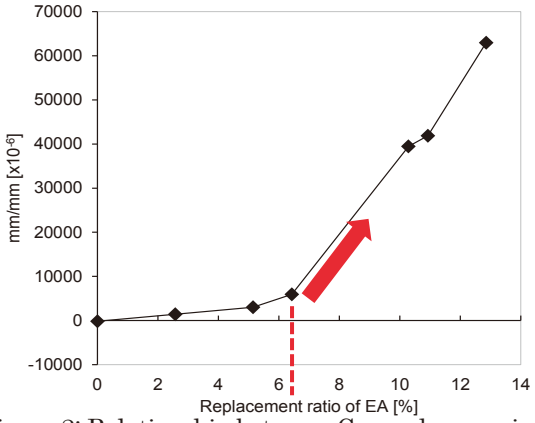

Figure 2: Relationship between C_{rep} and expansion strain at 7 days of age

3.4 Observation by micro-CT scanning

A cross-section image obtained by CT scanning is shown in Fig. 4, and a 3D image of a specimen of each C_{rep} is shown in Fig. 5. The cube in Fig. 5 has a side of 1 mm, which is approximately the same as the width of the specimen. The observation results in Photo 5 show that microcracks increase when the C_{rep} is 10.3% compared to 8.4%. Microcracks are radially generated from the aggregated portion of the hydration products. Hydration products such as these are not generated in the case of PC alone, and it is considered that the EA particles have grown. This result shows that the strength decrease is caused by the expansion of the EA particles themselves.

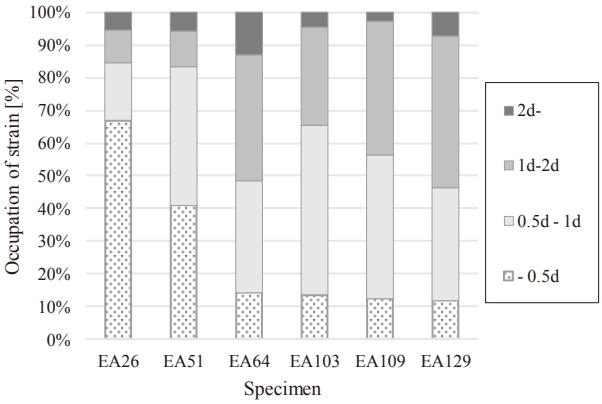

Figure 3: Expansion strain percentage of duration to 7 days of age

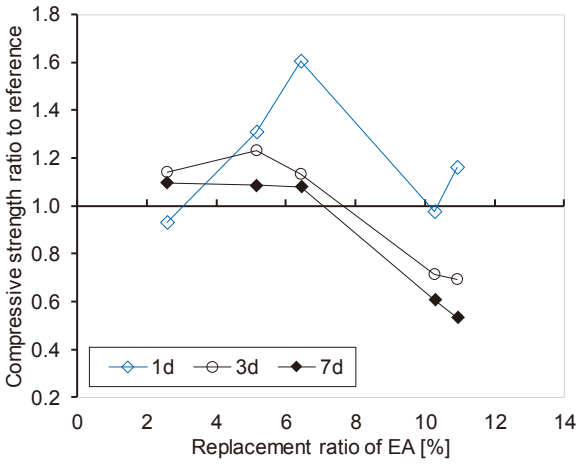

Figure 4: Relationship between C_{rep} and compressive strength

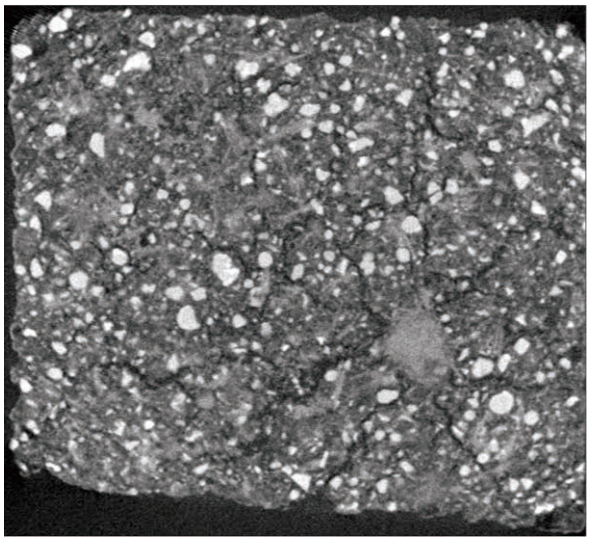

Figure 6: CT-scanning image of hardened cement paste bar (C_{rep} = 10.3%)

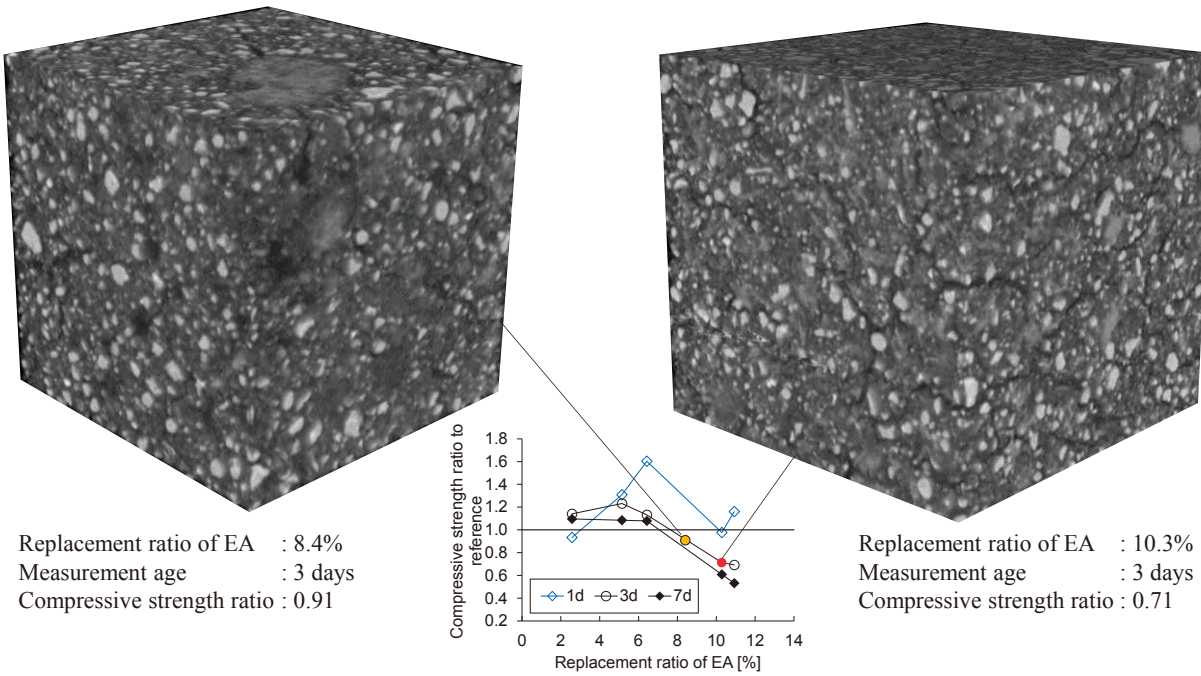

Figure 5: 3D CT-scanning image of hardened cement paste bar

3.5 Observation and elemental analysis by E-SEM

Fig. 7 shows BSE images of a raw EA particle, Fig. 8 and Fig. 9 show a hydrated EA particle at 3 days of age.

The EA particles have a structure in which f-CaO is the main constituent mineral, and the gaps are filled with C_3A, C_4AF, and anhydrite.

From Fig. 8, it can be confirmed that the precipitation position of each hydration product is the same as that of f-CaO, C_3A, and C_4AF, which are the origins of each product present in the raw EA particles. Therefore, it can be inferred that most minerals do not dissolve in solution and are converted to hydration products on the spot.

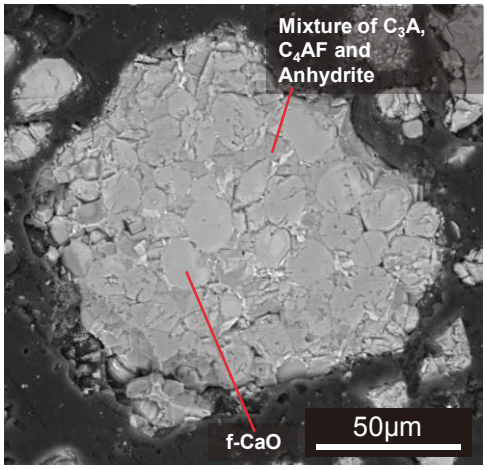

Figure 7: Raw EA particle

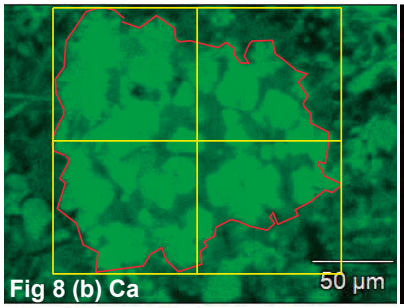

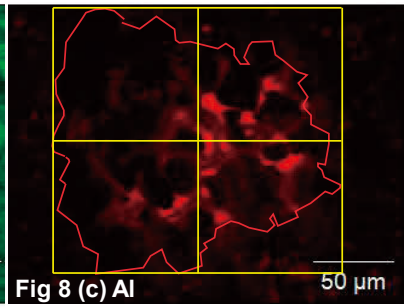

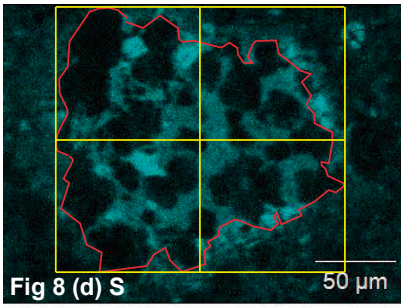

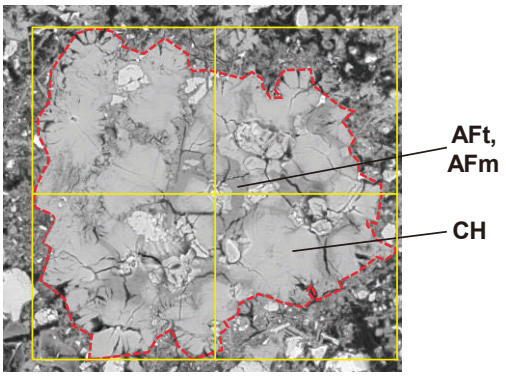

(a) BSE image of hydrated EA

Figure 8 (a)-(d): Element mapping images of hydrated EA particle

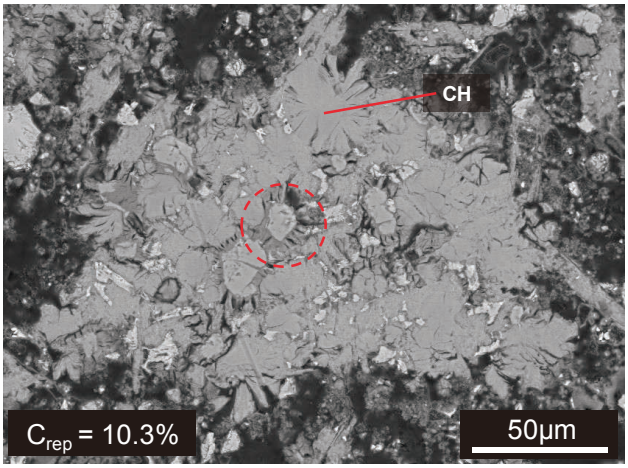

Figure 9: Hydrated EA particle at 3 days of age (C_{rep} = 10.3%)

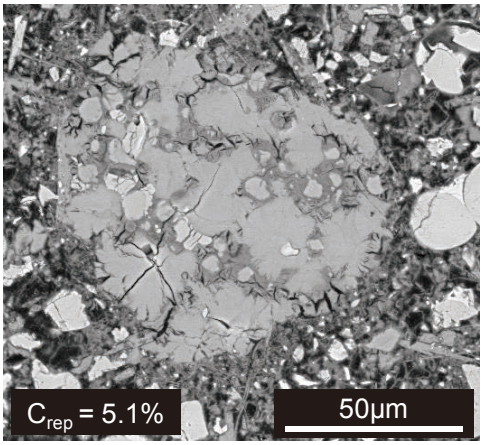

Figure 10: Hydrated EA particle at 3 days of age (C_{rep} = 5.1%)

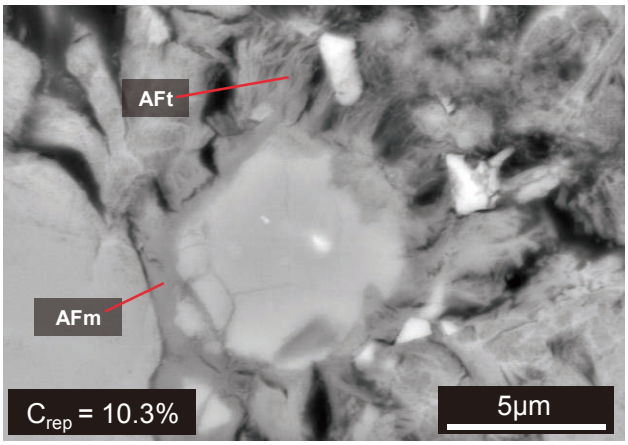

Figure 11: Ettringite and pores generated around C_3A in EA at 3 days of age

From observation results of EA C_{rep} = 10.3% (Fig. 9), we confirmed a larger amount of AFt was produced than in 5.1% (Fig. 10). (For example, a part surrounded by the red dash line in Fig. 9.) The enlarged image of the formation location of AFt is shown in Fig. 11. Mono-sulphate (AFm) exists on the surface of C_3A, and needle-like AFt grows vertically from above. In addition, a large quantity of pores formed simultaneously around the AFt. This result shows that rapid strain expansion occurring near C_{rep} exceeding 6.4% is caused by vertically generated AFt with pores. Also, as with Delayed Ettringite Formation, we have concluded that anhydrite dissolves in water once and AFt can be produced only when the sulphate ion concentration exceeds a certain threshold.

§4. CONCLUSIONS

- The expansion strain increases sharply when the replacement ratio of EA (C_{rep}) exceeds 6.4%.
- The setting time tended to be faster when the C_{rep} was up to 6.4%, but when the C_{rep} exceeded 6.4%, the setting time became slower as the C_{rep} increased.
- Compressive strength tended to decrease compared to reference when the C_{rep} exceeded 6.4%.
- From the cross-section image of C_{rep} 10.3% obtained by CT scanning, microcracks are radially generated from the aggregated portion of the hydration product. This result shows that the strength decrease is caused by the expansion of the EA particles themselves.
- From the image of the formation location of AFt in EA particles of C_{rep} 10.3% paste, AFm exists on the surface of C_3A, and needle-like AFt grows vertically from above. In addition, a large quantity of pores formed simultaneously around the AFt. This result shows that rapid strain expansion occurring near C_{rep} exceeding 6.4% is caused by this vertically generated AFt with pores. Also, as with Delayed Ettringite Formation, we have concluded that anhydrite dissolves in water once and AFt can be produced only when the sulphate ion concentration exceeds a certain threshold.

Acknowledgements

I would like to express my sincere gratitude to Associate Professor Guang Ye of Delft University of Technology and CMMB group members for much helpful advice, and technicians who supported the experiments.

REFERENCES

Journal Paper:

[1] Minoru MORIOKA, Yasuhiro NAKASHIMA, Takayuki HIGUCHI, Masataka EGUCHI, Etsuo SAKAI and Masaki DAIMON: 'Characteristics of Expansive Additives in the System of Free Lime-Hydraulic Compound-Anhydrite', Tokyo: Journal of the Society of Inorganic Materials, Japan, 2003, Vol. 10, 225-232

[2] Kenji YAMAMOTO, Minoru Morioka, Etsuo SAKAI and Masaki DAIMON: 'Expansion Mechanism of Cement Added with Expansive Additive', Tokyo: Concrete Research and Technology, 2003, Vol. 14, No. 3, 23-31

[3] Hyeonggil Choi, Heesup Choi, Myungkwan Lim, Takafumi Noguchi, Ryoma Kitagaki: 'Modeling of volume changes of concrete mixed with expansive additives', Construction and Building Materials, 2015, 266-274

Standards:

[4] JIS R 5210, Portland cement, 2009, 22 pages

[5] JIS R 5201, Physical testing methods for cement, 1997, 46 pages

[6] ASTM C191-13, Standard Test Methods for Time of Setting of Hydraulic Cement by Vicat Needle. West Conshokocken: American Society for Testing and Materials, 2013, 8 pages

Kohsuke Handa

Short comment

Understanding and modeling hydration mechanisms and microstructures will greatly help to predict concrete deterioration. I believe this to be the valuable perspective that cannot be obtained from macro experiments alone.